IEEE Access
Multidisciplinary | Rapid Review | Open Access Journal

Received May 4, 2022, accepted May 21, 2022, date of publication May 23, 2022, date of current version May 27, 2022.

Digital Object Identifier 10.1109/ACCESS.2022.3177603

Acoustic Based Localization of Partial Discharge Inside Oil-Filled Transformers

HAMIDREZA BESHARATIFARD[1], SAEED HASANZADEH[1], EHSAN HEYDARIAN-FORUSHANI[1], AND S. M. MUYEEN[2], (Senior Member, IEEE)

[1]Department of Electrical and Computer Engineering, Qom University of Technology, Qom 151937195, Iran
[2]Department of Electrical Engineering, Qatar University, Doha, Qatar

Corresponding authors: Saeed Hasanzadeh (hasanzadeh@qut.ac.ir) and S. M. Muyeen (sm.muyeen@qu.edu.qa)

This work was supported by Qatar National Library.

ABSTRACT This paper addresses the localization of Partial Discharge through a 3D Finite Element Method analysis of acoustic wave propagation inside a 3-phase 35kV transformer with the help of COMSOL Multiphysics software. Due to the complexity inside transformers, acoustic waves generated by PDs cannot simply be detected with typical acoustic sensors, especially when PDs happen inside inner windings. These waves are distorted and attenuated along with their propagation. The type, number, and position of sensors are essential factors in PD localization inside a transformer. A new installation arrangement of fiber-optic acoustic sensors inside the transformers is proposed with this information. This array of acoustic sensors has significant effects on PD localization accuracy and has immunity from on-site noise and interference; more importantly, they can be installed after transformer manufacturing. They are reachable if needed to be repaired or replaced. Several numerical studies have been carried out considering different PD source positions, and the Levenberge-Marquardt algorithm is employed for solving localization equations.

INDEX TERMS Acoustic signal propagation analysis, FEM simulation, Levenberg–Marquardt algorithm, partial discharge localization, power transformers.

ABBREVIATION

Electromagnetic interference	EMI
Signal to Noise Ratio	SNR
Finite Element Method	FEM
Generalized Minimal Residual Method	GMRES
High Frequency Current Transformers	HFCT
Time of Arrival	TOA
High Voltage Coupling Capacitors	HVCC
Ultra High Frequency	UHF
Partial Discharge	PD
Piezoelectric Transducer	PZT
Time Difference of Arrival	TDOA

I. INTRODUCTION

Power transformers are one of the most important and costly equipment in power systems. Based on transformer failure statistics in [1], the most common reason for failure in the power transformers is assigned to winding and insulation faults. Therefore, online monitoring of insulation systems of power transformers could avoid failures and catastrophic chain of events that lead to more destructions. One of the best ways to monitor transformers is PD measurement. PD in high voltage equipment is an electrical discharge in points with poor insulation or high electrical field. PD phenomenon has some electrical, electromagnetic, chemical, acoustic, and optical effects that can be detected with an appropriate type of sensor. In some studies, HFCTs, HVCCs, UHF Antennas, and acoustic sensors have been used for PD detection and measurement [2]–[8].

Due to the size of power transformers, PD measurement is not merely enough, and localization is needed to speed up fault detection and troubleshooting process. There are some challenges in PD localization in power transformers, such as choosing the type of sensors and their installation's position. Notably, the position of sensors is essential for achieving better accuracy. In some cases, UHF antennas and PZT sensors have been used for PD detection. These sensors could easily be influenced by the transformer's EMI and environment noises and interferences [9]–[11]. Commercial UHF sensors are costly, and the transformer's tank should be modified to install them [12], [13]. Typical acoustic methods could make

The associate editor coordinating the review of this manuscript and approving it for publication was Pavlos I. Lazaridis.

localization of PDs inside LV-winding or between winding and core difficult with typical acoustic methods [14]. The Fiber-Optic acoustic sensor array can be used to overcome the related problems of the conventional methods, such as on-site electromagnetic interference and noises, low sensitivity, faulty localization, and installation limitation.

These sensors should be closed to or even embedded inside the transformer's windings in order to receive less distorted PD signals. In [15], a new array has been introduced for sensor installation inside a single-phase transformer. However, this array cannot be used in transformers currently in service. It can only be installed during the manufacturing process of the transformer due to its installation position. The study of the acoustic pressure wave propagation path inside the transformer is crucial for the measurements and localization of the acoustic PD waves. [16], [17] analyzed the acoustic wave propagation within the transient state using numerical calculation. [18], [19] investigated the PD acoustic pressure wave distribution inside a transformer model. [20], [21] studied the PD acoustic pressure wave distribution inside a transformer using a simulation model and experimental results. Most of the previous papers that studied acoustic PD wave propagation inside transformers with FEM analysis did not present a comprehensive model of a real transformer. Recently, the authors have considered the transformer winding as an integrated cylinder, and in some of them, they modeled only the high voltage winding without the low voltage [18], [19]. Lack of recording the response of acoustic waves using the probe point feature at different points within the simulated model and lack of post-processing of collected data from FE software are other disadvantages of previous works [18], [19], [22], [23]. These papers solely focused on acoustic pressure wave distribution inside transformers and showed the acoustic pressure at different simulation times. In past years, fiber-optic acoustic sensors have been used in the laboratory, and real-world applications such as measurement and localization of PDs inside oil impressed transformers [15], [23], [29]. The placement of these sensors greatly affects the accuracy of localization.

In this paper, the acoustic localization of PD has been studied with finite element simulation of acoustic partial discharge wave propagation inside a transformer. A new array for sensor installation's position has been proposed. The advantage of this array is that sensors can be installed after transformer manufacturing, and they are reachable if needed to be replaced or repaired. A real 3-phase oil-filled transformer has been simulated in the COMSOL Multiphysics software environment.

Acoustic wave propagation inside the transformer has been analyzed with numerical methods. This paper simulates PDs as acoustic pressure sources in four positions, Case A and D inside LV-winding and Case B and C inside HV-winding. Eight sensors have been installed in one phase winding of the transformer as an observation point. Using FEM simulations, acoustic wave propagation has been solved numerically. PD signals originated from transformer winding are shielded, distorted, attenuated, and reverberated along with their propagation before reaching the sensors. Sensors closer to PD sources or direct paths to them receive signals with less distortion and attenuation and more SNR. With this array, at least four sensors can detect direct signals with acceptable SNR that can be used for localization. Arriving time of acoustic signals, also known as the TOA, has been used in some cases. Sufficient accuracy, immunity from on-site noise and interference, and accessibility are advantages of this array of acoustic sensors. This method's localization of PDs requires a PD propagation time reference measured by electrical or UHF methods [30]–[32]. TDOA between received signals among all the sensors in the array, initiated from the same PD acoustic source, can be used for localization instead, and it can be carried out independently with acoustic sensors [33]–[35]. Localization equations have been formed and solved with the Levenberge-Marquardt algorithm Using FEM simulation results and the TDOA method [36]. The main contributions of this work are:

- Conducting a comprehensive 3D model of a real-size 3-phase oil-filed 35kV transformer.
- Proposing a new array of fiber-optic acoustic sensors for installation inside existing oil-filled power transformers that enables high accuracy PD localization.
- Studying the full in-depth study of acoustic PD phenomenon using finite element analysis.

This paper is organized as follows: Section II describes the analysis of acoustic wave propagation inside a 3D model of a 3-phase transformer using FEM simulations. The proposed sensor array and localization results are presented and discussed in Section III. In section IV, a new case study is presented to verify localization results, and section V reports the conclusions of this paper.

II. FINITE ELEMENT-BASED ANALYSIS OF ACOUSTIC WAVE PROPAGATION

The first step for finite element simulations is building a 3D model of the transformer. This 3D model is based on a real-size 3-phase oil-filed 35kV transformer. The geometry of the model is shown in Fig. 1. Moreover, the dimensions are shown in Table 1 [15]. The transformer tank has been filled with oil, the fluid model is linearly elastic, and the oil temperature is 20°C. Three iron cores have been surrounded by the low voltage and the high voltage windings. The transformer core, transformer yoke, and tank material are steel for structural and copper for windings. The materials inside the transformer tank have been assigned to insulation oil, the transformer core, and windings. By adding the material from the software library, these materials' properties will be automatically added to the transient pressure acoustic module. The software predefined the relative permeability of the structural steel, the relative permittivity of the copper, the thermal conductivity of the oil, and other properties of the materials. Some properties of the material, such as material density and the speed of the sound inside them, need to

TABLE 1. Transformer dimension.

Parameter	Size (m)
Outer radius of HV winding	0.25
Inner radius of HV winding	0.19
Outer radius of LV winding	0.13
Inner radius of LV winding	0.1
Transformer winding height	0.6
Transformer tank dimensions	2.4×0.8×0.8
Iron core height/radius	0.6×0.1
Transformer yoke dimensions	1.6×0.05×0.2
Disk winding thickness	0.04

TABLE 2. Properties of the materials.

Material	Density (kg/m3)	Sound speed (m/s)	Young's modulus (Pa)
Structural Steel	7850	5100	200 e^9
Copper	8700	4760	110 e^9
Insulation oil	890	1420	14 e^9

TABLE 3. Properties of the predefined materials.

Properties	Unit	Structural Steel	Copper
Relative permeability	1	1	1
Thermal conductivity	W/(m×K)	44.5	400
Electrical conductivity	S/m	4.03e^6	5.99e^7
Relative permittivity	1	1	1
Poisson's ratio	1	0.3	0.35
Coefficient of thermal expansion	1/K	12.3e^{-6}	17e^{-6}
Heat capacity at constant pressure	J/(kg×K)	475	385

be defined, shown in Table 2 [15]. Some of the predefined properties of the material in the software are shown in Table 3.

A transient pressure acoustic module has been chosen for modeling the acoustic wave propagation caused by the PD source inside the transformer. With the help of COMSOL Multiphysics, acoustic pressure physic law could easily be applied to the model.

For acoustic pressure analysis, materials have been assumed to be isentropic, which means they are lossless and adiabatic. Also, the material density and the sound speed can be assumed constant and isotropic. The momentum equation and the continuity equation for isotropic fluid flow are extracted from [15]:

$$\frac{\partial \bar{\mathrm{v}}}{\partial t} + (\bar{\mathrm{v}} \cdot \nabla)\ \bar{\mathrm{v}} = -\frac{1}{\rho}\nabla \mathrm{P} \tag{1}$$

$$\frac{\partial \rho}{\partial t} + \nabla \cdot (\rho \vec{\mathrm{v}}) = 0 \tag{2}$$

where $\bar{\mathrm{v}}$ is the velocity field. ρ is the total density, and P is the total pressure. The compressibility of liquids can be stated:

$$C = \sqrt{\frac{\mathrm{B}}{\rho}} \tag{3}$$

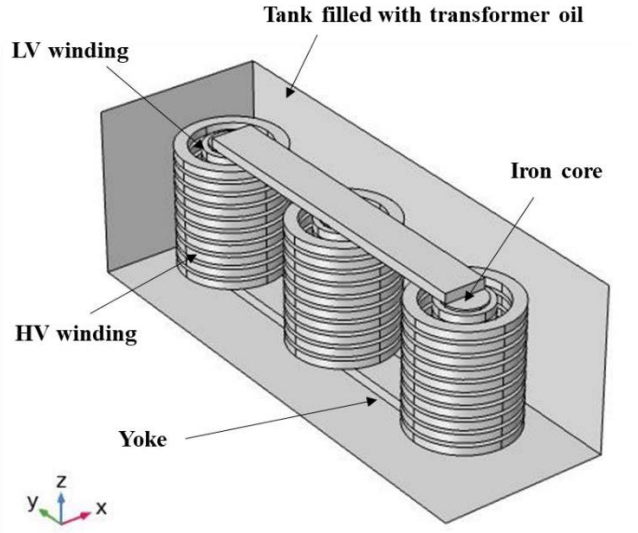

FIGURE 1. 3D model of the transformer.

where B is the bulk modulus, and C is the speed of sound inside the liquid. For acoustic propagation study driven by PD events, all the variables can be treated as just small perturbations around their stationary quiescent values [15]:

$$\begin{aligned} P &= P_0 + \Delta P \\ \rho &= \rho_0 + \Delta \rho \\ \mathrm{v} &= 0 + \Delta \mathrm{v} \end{aligned} \tag{4}$$

After inserting these extensions into the governing equations, with Taylor expansion, if necessary, reshuffling and dropping the minor variations can yield the wave equation for sound waves [15]:

$$\frac{1}{\rho c^2}\frac{\partial^2 P}{\partial t^2} - \nabla \cdot \left(-\frac{1}{\rho}(\nabla P - q_d)\right) = \mathrm{Q}_m \tag{5}$$

where ρc^2 (N/m^2) is recognized as bulk modulus, the dependent variable in the wave equation is the sound pressure, P. The sound pressure is propagating in a medium with density at the speed of sound, C. The q_d and Q_m represent the dipole and monopole domain sources. A monopole domain source can be described as a small pulsating sphere, contracting and expanding with time. In other words, the monopole source radiates sound equally in all directions.

On the other hand, a dipole source is made up of two identical monopole sources in opposite phases and separated by a minimal distance compared to the wavelength of sound. The continuity boundary condition is applied to all the transformer model's inner boundaries, and the transformer tank's outer boundaries have been defined as impedance. PDs inside the transformer have the main frequency between 20 kHz to 500 kHz [14]. The acoustic PD source is like a damped sine wave. The monopole acoustic source behavior is close to a PD event, so the PD source has been defined as a monopole

TABLE 4. The mesh grid statistics.

Mesh vertices	29808
Tetrahedral	175054
Triangles	36564
Edge elements	8946
Vertex elements	974

Domain element statistics

Domain element statistics	0.6
Number of elements	175054
Minimum element quality	0.05583
Average element quality	0.6255
Element volume ratio	$7.335e^{-5}$
Mesh volume	1.536 m^3

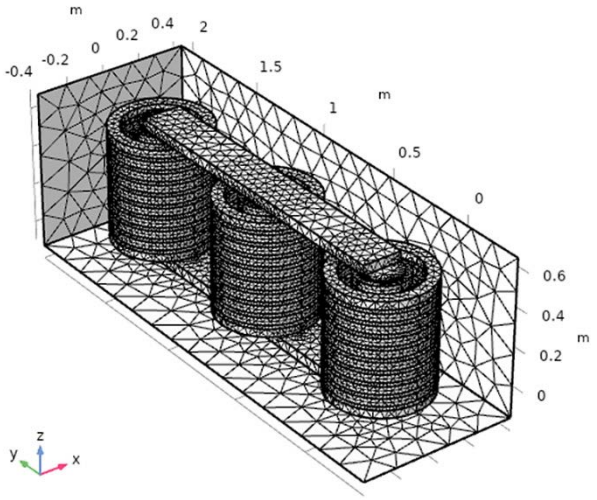

FIGURE 2. Mesh grid of the 3D model.

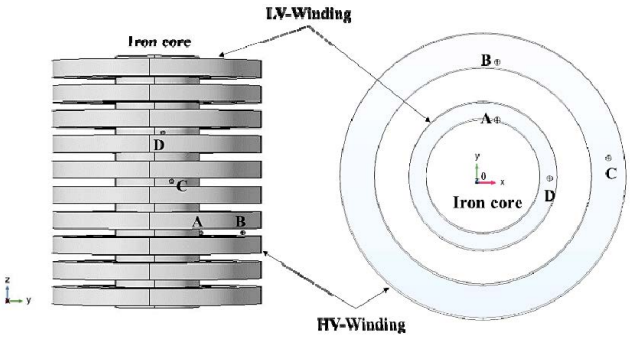

FIGURE 3. Position of four PD sources inside transformer windings.

domain source, and it can be described with:

$$Q_m(\mathrm{t}) = A_q \mathrm{e}^{-t/\tau} \sin(2\pi \mathrm{f\,t}) \tag{6}$$

where f is the acoustic wave frequency produced by PD, 20 kHz; in this study, A_q is the flow of energy and is set as a constant ($A_q = 1$). The decay of the acoustic wave, τ, is equal to 50 μs and the acoustic wave dies after 200 μs. The suggested iterative solver by the software is the GMRES solver. The GMRES method is an iterative method for the numerical solution of an indefinite nonsymmetrical system of linear equations. The GMRES solver with the Geometric multigrid preconditioner ensures low memory consumption at a high mesh resolution. In the simulation, the GMRES linear system solver with a geometric multigrid preconditioner is applied for transient analysis with a time step of 1 μs. The study has been carried out 1000 μs time duration after PD happens. The divided mesh grid consisted of 175054 tetrahedral elements, and the minimum element quality is 0.05583 m, as shown in Fig. 2 and Table 4. Simulations have been carried out for different PD source positions, Case A and D inside LV-winding and Case B and C inside HV-winding, and it is shown in Fig. 3.

From Fig. 3, it is obvious that the center of the cylindrical iron core is selected as the origin point of the X and Y axis, while the origin point of the Z-axis is set in the plane, which is defined by the circular bottom surface of the cylindrical iron core. The acoustic wave propagates outward from the PD source through spherical waves inside the transformer as the lossless propagation process gets further attenuated toward receivers. This can be demonstrated in Fig. 4; total acoustic pressure originating from the PD source in point A has been shown in 200, 500, and 1000 μs after propagation. In Fig. 4, the intensity of the acoustic pressure field is demonstrated by the color map. It can be seen that the acoustic pressure amplitude has decreased over time as the acoustic wave travels away from the PD source. When a PD happens inside a transformer, the acoustic wave spreads through the medium, and with the total energy of the acoustic wave being constant, an increase in diffusion distance results in decreasing of energy per unit area with the square of the distance from the acoustic source (i.e., diffusive attenuation). Refraction and reflection will occur during the propagation of the acoustic waves through the windings and the iron core, and the acoustic signals will reverberate. The speed of sound in the iron core and the windings is faster than in the oil. So, the signals propagate faster in the windings, core, and other mediums than in the oil. But the attenuation in the windings and core is greater, which is consistent with the theory of acoustic wave propagation.

III. PROPOSED SENSOR ARRAY DESIGN AND LOCALIZATION OF DIFFERENT PD SOURCES

When PD occurs inside the transformer, the acoustic waves originating from the PD source can be detected and measured with acoustic sensors. Eight observation points have been defined as sensors on the top and bottom of one phase of transformer winding. These observation points/probe points are referred to as sensors in the text for ease. Four sensors have been placed at the bottom of the HV-Winding. Four sensors have been placed on the top of HV-Winding with a 45-degree clockwise shift, respectively, from the sensors placed below them. The coordinate for the position of the

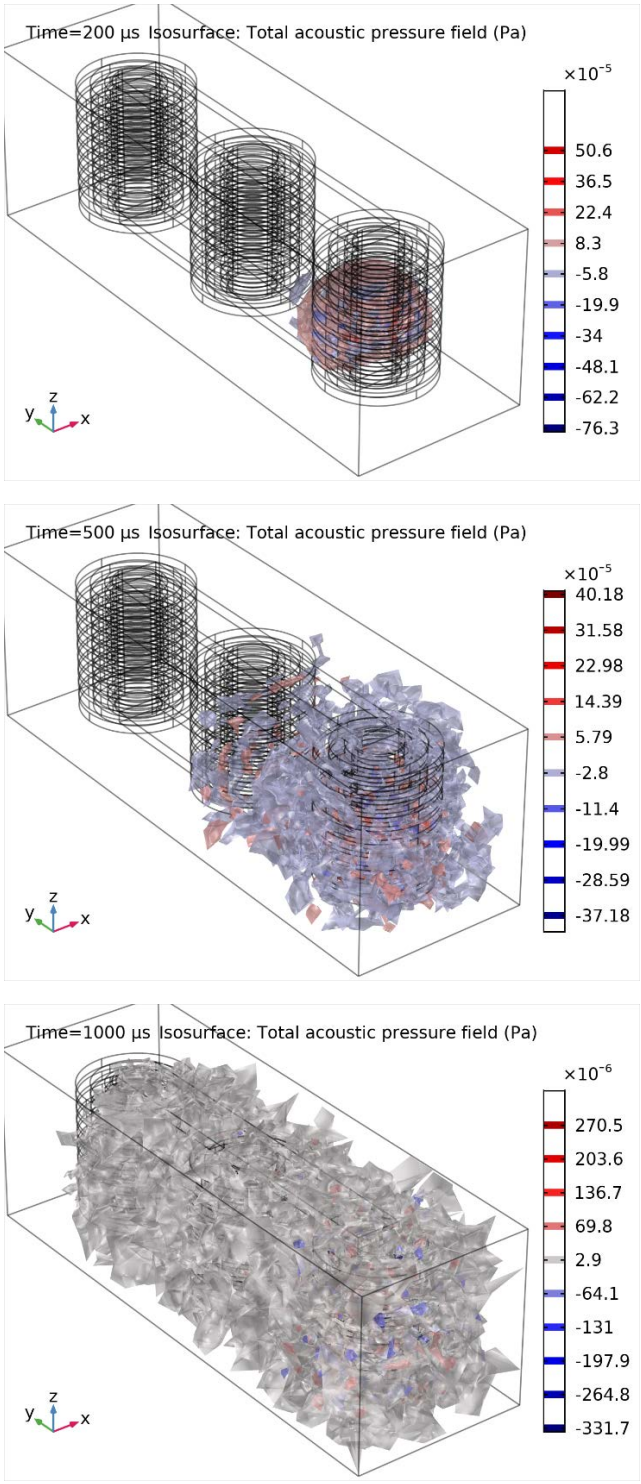

FIGURE 4. Total acoustic pressure originated from the PD source placed in point A at 200 μs, 500 μs, and 1000 μs after propagation.

sensors is given in Table 5. One of the important factors in PD localization is finding the arrival time of PD to each sensor. PDs that are closer to sensors or have a direct pass to them are less distorted and attenuated; as a result, they arrive faster at the sensors. TOA determines which sensor has more SNR and which received signal is closer to its original form. SNR is an essential factor in acoustic wave

TABLE 5. The coordinate for the proposed sensor array.

Number of sensors	Coordinates (m)
#1	(0.188, 0, 0)
#2	(0.133, -0.133, 0.6)
#3	(0, -0.188, 0)
#4	(-0.133, -0.133, 0.6)
#5	(-0.188, 0, 0)
#6	(-0.133, 0.133, 0.6)
#7	(0, 0.188, 0)
#8	(0.133, 0.133, 0.6)

propagation analysis [14]. Due to placing sensors inside the transformer, white noise and other on-site noise and interference are shielded and blocked by the transformer tank. However, the impulse sound originating from the changing size and orientation of magnetic domains in the core material, the so-called Barkhausen noise, reaches well into several tens of kHz and can affect the measurement. It is possible to nullify many of these effects that are not associated with PDs by using a band-pass filter. These noises include vibrations caused by the magnetostrictive action of the core (Barkhausen noise), pumps, and fans. Most of these noises are below 30 kHz; however, the Barkhausen noise emanating from the core has sometimes been found to be in the 50 kHz range [14]. The distance between sensors causes a delay in time arrival of PD signals. By having the position of sensors and calculating the TDOA between sensors, PD localization is possible. For this purpose, four out of eight sensors that have acceptable SNR and are less distorted could be chosen for localization.

For the PD source in position A, the acoustic signal arriving at sensors 7, 1, 5, and 8 have been shown in Fig. 5. The TOA for these sensors is less than others, so it could be concluded that these sensors receive signals with less vibration and distortion or are closer to the PD source to be used for localization. It is evident for the PD source in position A that the acoustic PD signals need to penetrate the core and the LV-Winding to reach the sensors 2, 3, 4. As a result, signals have a lower amplitude in the first cycles because of reflection and vibration, and they have low SNR. These acoustic signals contain information for all the distance the wave travels through different mediums after several unpredicted reflections, so these observation points cannot be used for localization. By choosing the sensor with the least TOA as a reference, the TDOA to sensors 1, 5, and 8 is 48 μs, 78 μs, and 190 μs. Absolut TOA for sensors 2, 3, 4, and 6 is 434 μs, 385 μs, 474 μs, and 379 μs, and it is shown in Fig. 6. The distance between each sensor to PD source is given by [37]:

$$D_i = v_s T_i \tag{7}$$

where D_i is the distance between the sensor and PD source location, v_s is the speed of sound in the oil, and T_i is the measured arrival time of the PD signal. The sound speed in the oil in the equations is 1400 m/s at 20 °C. The propagation speed goes down to about 1200 m/s for transformer mineral oil at 80 °C. In order to compare the result of our work

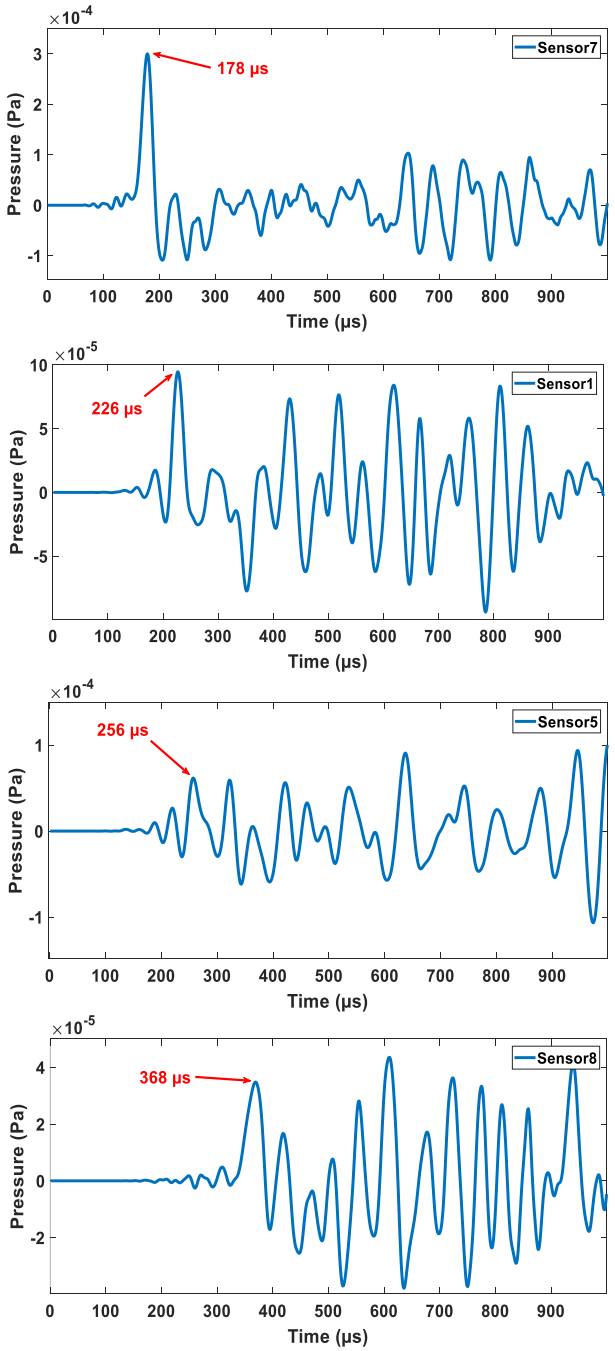

FIGURE 5. Acoustic signals originated from source A received by sensors 7, 1, 5, and 8.

with previous works, we assume that the oil temperature is 20°C [15]. If the PD coordinate is (x, y, z) and the sensors coordinate is defined as (x_{ai}, y_{ai}, z_{ai}), localization equations can be described as:

$$\begin{aligned}
&(x - x_{a1})^2 + (\mathrm{y} - y_{a1})^2 + (\mathrm{z} - z_{a1})^2 = (v_s.T_1)^2 \\
&(x - x_{a2})^2 + (\mathrm{y} - y_{a2})^2 + (\mathrm{z} - z_{a2})^2 = (v_s.T_2)^2 \\
&\ldots. \\
&(x - x_{ai})^2 + (\mathrm{y} - y_{ai})^2 + (\mathrm{z} - z_{ai})^2 = (v_s.T_i)^2
\end{aligned} \tag{8}$$

In (8), T_i cannot be measured by acoustic sensors due to the time delay of these sensors in the range of micro or millisecond; for measuring the real PD propagation time, PD measurement with an electrical or UHF method is needed. Electrical or electromagnetic PD pulses (generated from PD source) arriving time to electric or UHF sensors is in the range of Nanoseconds. It is close to the signal's real-time propagation to be used as a time reference for acoustic signals.

In this paper, localization has been carried out only with acoustic sensors, so TOA is unsuitable, and TDOA could be used instead. In the time-difference approach, assuming straight propagation, the acoustic wave reaches the nearest sensor first and triggers the recording process on all sensors simultaneously. So, for this purpose, sensor7 has been chosen as a time reference, and the TDOA has been calculated and respected by sensor7. Another form of the (8) has been written:

$$\begin{aligned}
&\sqrt{(x - x_{ai})^2 + (\mathrm{y} - y_{ai})^2 + (\mathrm{z} - z_{ai})^2} \\
&\quad - \sqrt{(x - x_{a1})^2 + (\mathrm{y} - y_{a1})^2 + (\mathrm{z} - z_{a1})^2} = v_s(T_i - T_1)
\end{aligned} \tag{9}$$

with $T_i - T_1 = \tau_{i1}$ non-linear equations, (9) can be solved with the help of the Levenberge-Marquardt algorithm and by trying certain initial guesses. Lower and upper bounds have been assigned for variables to avoid false localization like PD source solutions outside the transformer tank.

Localization error could be described with:

$$\Delta R = \sqrt{(x_{ac} - x)^2 + (\mathrm{y_{ac}} - y)^2 + (\mathrm{z_{ac}} - z)^2} \tag{10}$$

where (x_{ac}, y_{ac}, z_{ac}) is calculated PD source position with localization algorithm. PD localization for four PD source positions has been calculated, and the results have been shown in Table 6. The proposed sensor array and the PD localization results for Case A are shown in Fig. 7. In Case B, sensors 7, 1, 5, and 8 have been chosen for localization, and the absolute TOA for these sensors is 174, 244, 275, and 345 μs. The localization method, in general, uses the time-of-flight method for finding the source of acoustic signals. By assuming these captured acoustic signals have a straight pass from the acoustic source through the oil to the sensors, it is possible to form the equation and solve them using an optimization algorithm. However, this is feasible if the signal has high SNR and is clean (not distorted/reverberated) in the first cycles, as explained before. This shows the importance of the type of the sensor and the sensor installation position in capturing signals and the localization of PDs. For conventional acoustic emission sensors placed on the transformer's outside wall, this method suffers from significant uncertainties and potentially misleading results.

This is because of the differences in wave propagation through the tank wall and the liquid. Furthermore, the wave may take other, longer paths to a remote sensor or perhaps not reach the sensor at all due to blockage. Second, in reality, the tank wall is a thick steel plate, which, by its nature, has

TABLE 6. Localization results for all four study cases.

Case	PD Source Location(m)	TDOA From Simulations(μs)	PD Localization Results(m)	ΔR(cm)
A	(0.025, 0.107, 0.179)	τ_{71}=48, τ_{75}=78, τ_{78}=190	(0.0307, 0.109, 0.1608)	1.91
B	(0.025, 0.207, 0.179)	τ_{71}=70, τ_{75}=101, τ_{78}=171	(0.0375, 0.1688, 0.1942)	4.29
C	(0.215, 0.049, 0.302)	τ_{18}=6, τ_{12}=27, τ_{17}=60	(0.1959, 0.0371, 0.3053)	2.27
D	(0.113, 0.022, 0.417)	τ_{82}=24, τ_{86}=105, τ_{81}=175	(0.1501, 0.0269, 0.4349)	4.35

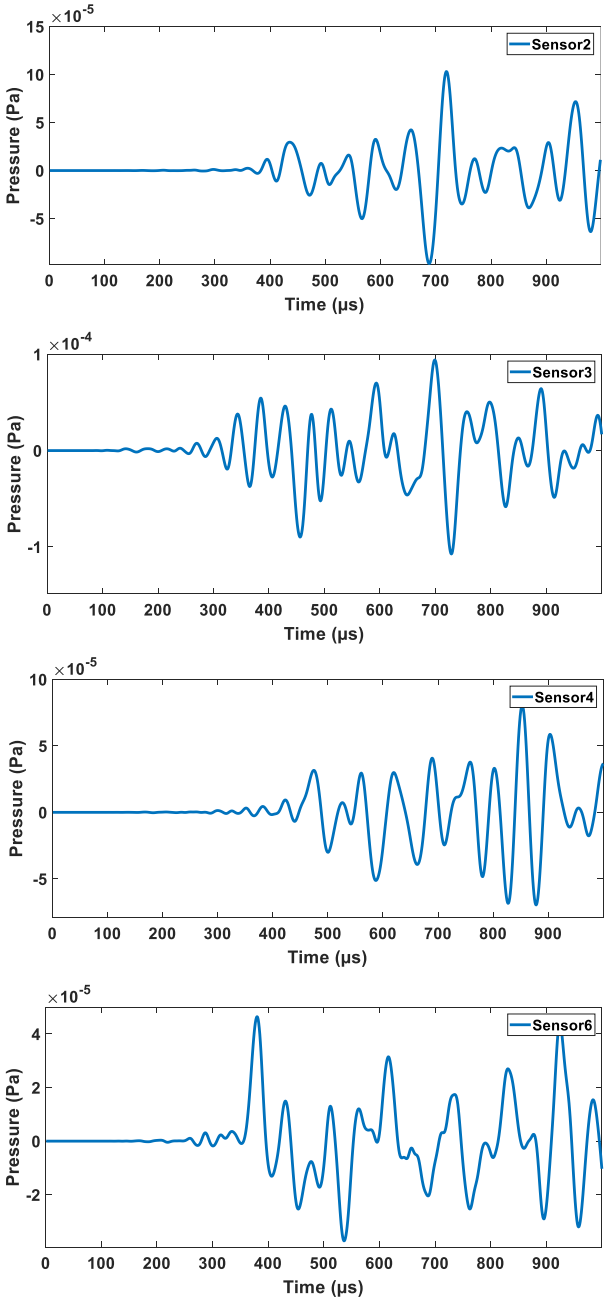

FIGURE 6. Acoustic signals arriving at sensors 2, 3, 4, and 6.

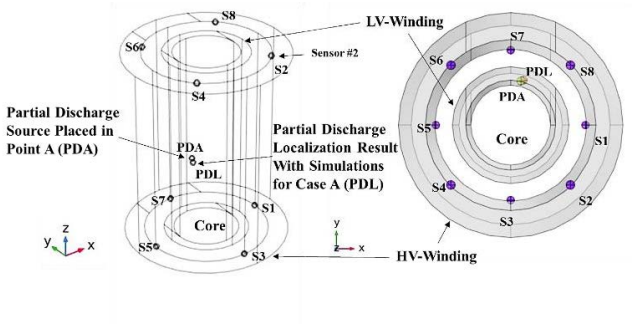

FIGURE 7. PD localization result for case A.

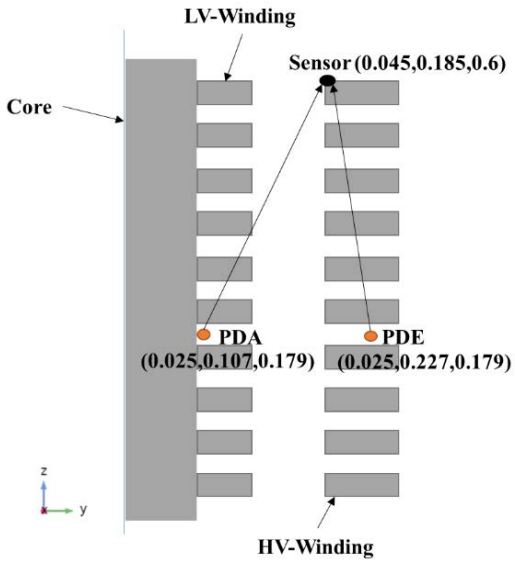

FIGURE 8. Acoustic signals propagation through transformer windings.

faster sound transmission properties than the insulating liquid [14]. These issues can be avoided by using the proposed array of fiber-optic acoustic sensors used in this study that most likely capture direct, clean, and non-distorted acoustic signals. In this research, factors such as the placement of the sensor, the calculation of the signal arrival time, the localization equations, and the optimization algorithm can affect the localization error. Table 6 shows that the proposed array of the acoustic sensor and the used localization equations alongside the optimization algorithm leads to acceptable localization accuracy. In real applications, in addition to the previous factors, localization accuracy depends on other factors such as the on-site noises and interference, the type of the sensor, the

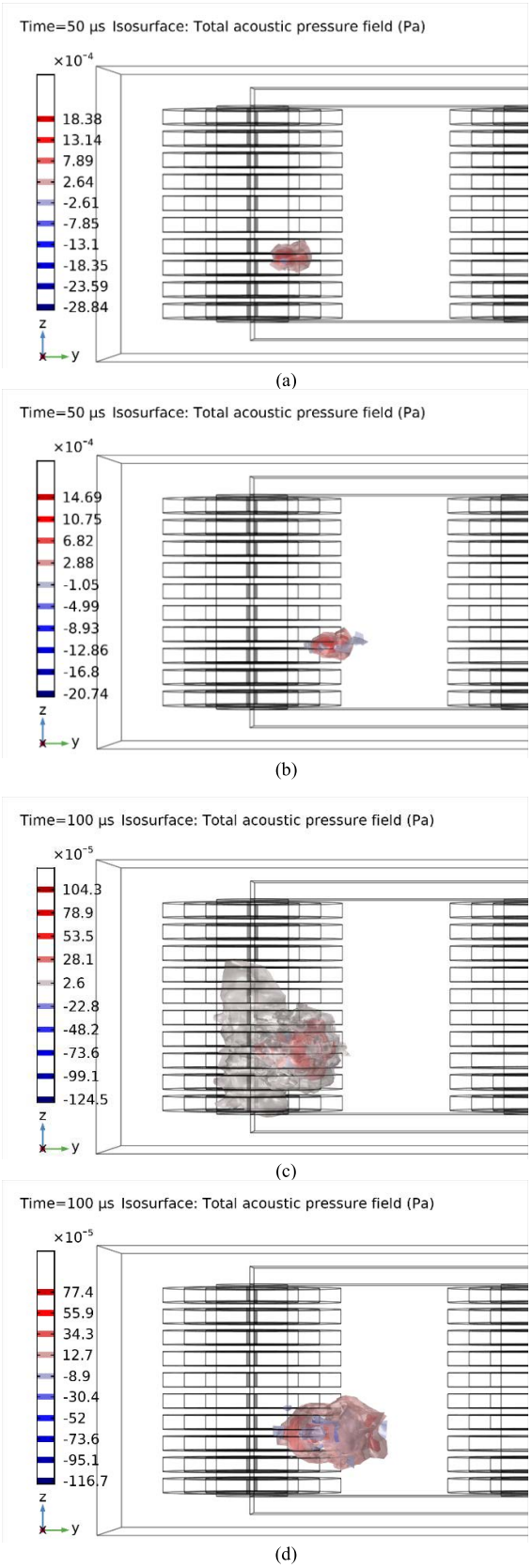

FIGURE 9. Total acoustic pressure originated from the PD source placed (a) in point A and (b) E at 50 μs after propagation and (c) in point A and (d) E at 100 μs after propagation.

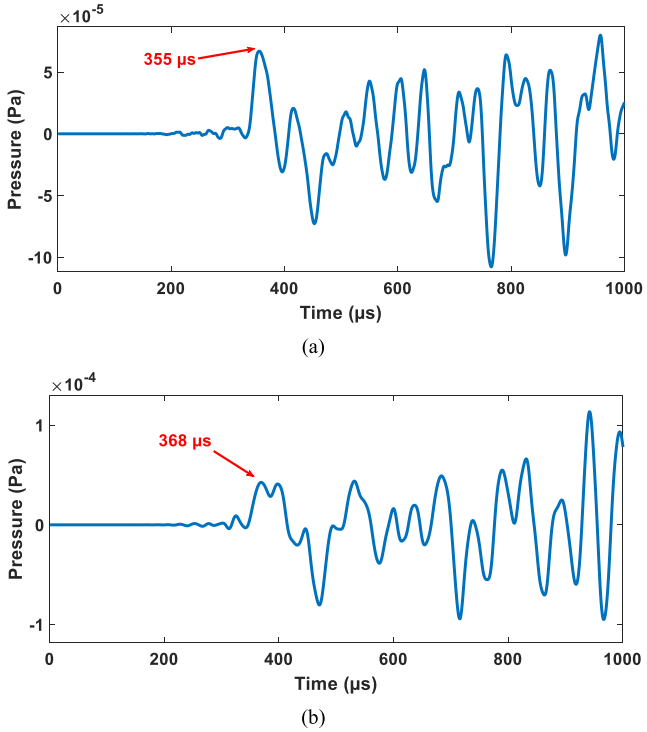

FIGURE 10. Captured acoustic signals generated from PD source, (a) in point A (PDA) and (b) E (PDE).

sensor sensitivity, the sensor bandwidth, and the complexity inside the transformer under test.

IV. A NEW CASE STUDY FOR VERIFICATION OF LOCALIZATION RESULTS

A new case study has been investigated to better understand the sensor's installation position importance and localization accuracy factors, where a PD source is defined at point E, and acoustic signal propagating from this source is compared with the PD source placed in point A. A new sensor is placed in coordinate (0.045, 0.185, 0.6), and for a better look, a 2D cut-plane view of the transformer winding and the core is shown in Fig. 8. The total acoustic pressure originating from the PD source in points A and E has been shown in Fig. 9 at 50 μs and 100 μs after propagation time. The captured signals from points A and E by this sensor are shown in Fig. 10.

In Fig. 8, by comparing the pass of acoustic signal propagation to the sensor, the acoustic signal from Case E needs to penetrate layers of the winding disk to reach the sensor. However, in Case A, the pass of the signal to the sensor is much more direct. As a result, For Case A, the signal's amplitude is higher, the absolute arrival time of the signal is lower than in Case E, and the signal is much cleaner (less distorted and vibrated) in the first cycles. However, the PD source in point E is closer to the sensor than the PD source placed in position A, but the sensor position and the pass of signal to the sensor have much more effect on PD localization accuracy. So, for those PDs inside windings, the

generated acoustic signals from them are more attenuated and reverberated along the way, the SNR is low, and localization error would be higher as the results of Table 6 could conclude.

V. CONCLUSION

In this paper, a novel structure array of fiber-optic acoustic sensors has been proposed for installation inside oil-filled power transformers. By using the acoustic module of COMSOL Multiphysics software, the performance of this array has been investigated inside a 3D model of a real 3-phase 35kV transformer. Using FEM simulation results and the TDOA method, localization equations have been formed and solved with the Levenberge-Marquardt algorithm. The analysis has been carried out for different PD source positions. The main conclusions and achievements of this work are:

1. When acoustic signals propagate inside an oil-impressed transformer, complex structures such as the transformer yoke, iron core, and windings affect the propagation path of the acoustic signals. A direct and non-distorted signal can be captured by placing the sensors close to or even embedded in windings. The direct acoustic signals most likely pass through the oil and reach the sensors with less attenuation or reverberation.
2. Using the proposed sensor's array, precise localization for a single PD event at any possible positions, including inside the low or high voltage windings or between the oil ducts, is achievable. The proposed array of acoustic sensors enables the localization of PDs inside transformers with less than 5 cm error.
3. Another advantage of the proposed array is that sensors can be installed inside existing oil-filled transformers, and they are reachable if needed to be repaired or replaced.

Acceptable accuracy, immunity from on-site noise and interference, and accessibility are the main advantages of this array of acoustic sensors. Due to study limitations, confirming the results with an experimental study wasn't feasible. The results of this paper can be helpful in acoustic PD localization inside power transformers with Fiber-Optic sensors.

REFERENCES

[1] *Transformer Reliability Survey*, Technical Brochure 642, Study Committee A2, WG A2.37, CIGRE, Paris, France, 2015.
[2] R. Liao, C. Guo, K. Wang, Z. Zuo, and A. Zhuang, "Adaptive optimal kernel Time–Frequency representation technique for partial discharge ultra-high-frequency signals classification," *Electr. Power Compon. Syst.*, vol. 43, no. 4, pp. 449–460, Feb. 2015.
[3] M. S. Naderi, T. R. Blackburn, B. T. Phung, M. S. Naderi, R. Ghaemmaghami, and A. Nasiri, "Determination of partial discharge propagation and location in transformer windings using a hybrid transformer model," *Electr. Power Compon. Syst.*, vol. 35, no. 6, pp. 607–623, Mar. 2007.
[4] R. Sarathi, V. Dubey, and Y. G. Srinivasa, "Characterization of partial discharges in a gas insulated system using an acoustic emission technique," *Electr. Power Compon. Syst.*, vol. 34, no. 6, pp. 653–669, Jun. 2006.
[5] R. Umamaheswari and R. Sarathi, "Identification of partial discharges in gas-insulated switchgear by ultra-high-frequency technique and classification by adopting multi-class support vector machines," *Electr. Power Compon. Syst.*, vol. 39, no. 14, pp. 1577–1595, 2011.
[6] M. Kunicki, A. Cichoń, and S. Borucki, "Measurements on partial discharge in on-site operating power transformer: A case study," *IET Gener., Transmiss. Distrib.*, vol. 12, no. 10, pp. 2487–2495, May 2018.
[7] F. Álvarez, F. Garnacho, J. Ortego, and M. Á. Sánchez-Urán, "Application of HFCT and UHF sensors in on-line partial discharge measurements for insulation diagnosis of high voltage equipment," *Sensors*, vol. 15, no. 4, pp. 7360–7387, Apr. 2015.
[8] H. Besharatifard, S. Hasanzadeh, E. Heydarian-Forushani, H. H. Alhelou, and P. Siano, "Detection and analysis of partial discharges in oil-immersed power transformers using low-cost acoustic sensors," *Appl. Sci.*, vol. 12, no. 6, p. 3010, Mar. 2022.
[9] A. Cavallini, X. Chen, G. C. Montanari, and F. Ciani, "Diagnosis of EHV and HV transformers through an innovative partial-discharge-based technique," *IEEE Trans. Power Del.*, vol. 25, no. 2, pp. 814–824, Apr. 2010.
[10] H. Zhang, T. R. Blackburn, B. T. Phung, and D. Sen, "A novel wavelet transform technique for on-line partial discharge measurements. 2. On-site noise rejection application," *IEEE Trans. Dielectr. Electr. Insul.*, vol. 14, no. 1, pp. 15–22, Feb. 2007.
[11] H. Zhang, T. R. Blackburn, B. T. Phung, and D. Sen, "A novel wavelet transform technique for on-line partial discharge measurements. 1. WT denoising algorithm," *IEEE Trans. Dielectr. Electr. Insul.*, vol. 14, no. 1, pp. 3–14, Feb. 2007.
[12] M. D. Judd, L. Yang, and I. B. B. Hunter, "Partial discharge monitoring for power transformer using UHF sensors. Part 2: Field experience," *IEEE Elect. Insul. Mag.*, vol. 21, no. 3, pp. 5–13, May/Jun. 2005.
[13] M. D. Judd, G. P. Cleary, C. J. Bennoch, J. S. Pearson, and T. Breckenridge, "Power transformer monitoring using UHF sensors: Site trials," in *Proc. Conf. Rec. IEEE Int. Symp. Electr. Insul.*, Apr. 2003, pp. 145–149.
[14] *IEEE Guide for the Detection, Location and Interpretation of Sources of Acoustic Emissions From Electrical Discharges in Power Transformers and Power Reactors*, IEEE, Piscataway, NJ, USA, 2019.
[15] C. Gao, L. Yu, Y. Xu, W. Wang, S. Wang, and P. Wang, "Partial discharge localization inside transformer windings via fiber-optic acoustic sensor array," *IEEE Trans. Power Del.*, vol. 34, no. 4, pp. 1251–1260, Aug. 2019.
[16] D. Wotzka, T. Boczar, and P. Fracz, "Mathematical model and numerical analysis of AE wave generated by partial discharges," *Acta Phys. Polonica A*, vol. 120, no. 4, pp. 767–771, Oct. 2011.
[17] D. Wotzka, D. Zmarzły, and T. Boczar, "Numerical simulation of acoustic wave propagating in a spherical object filled with insulating oil," *Acta Phys. Polonica A*, vol. 118, no. 6, pp. 1272–1275, Dec. 2010.
[18] D. Wotzka, T. Boczar, and D. Zmarzły, "Analysis of acoustic wave propagation in a power transformer model," *Acta Phys. Polonica A*, vol. 116, no. 3, pp. 428–431, Sep. 2009.
[19] D. Wotzka, "Partial discharge simulation in an acoustic model of a power transformer," in *Proc. 2nd Int. Students Conf. Electrodyn. Mechatronics*, May 2009, pp. 39–40.
[20] A. O. Akumu, N. Kawaguchi, R. Ozaki, H. Ihori, M. Fujii, and K. Arii, "A study of partial discharge acoustic signal propagation in a model transformer," in *Proc. Int. Symp. Electr. Insulating Mater. (ISEIM), Asian Conf. Electr. Insulating Diagnosis (ACEID), 33rd Symp. Electr. Electron. Insulating Mater. Appl. Syst.*, Nov. 2001, pp. 583–586.
[21] A. O. Akumu, F. Adachi, N. Kawaguchi, R. Ozaki, H. Ihori, M. Fujii, and K. Arii, "A 3-D numerical simulation of partial discharge acoustic wave propagation in a model transformer," in *Proc. Conf. Rec. IEEE Int. Symp. Electr. Insul.*, Apr. 2002, pp. 183–186.
[22] S. N. Meitei, K. Borah, and S. Chatterjee, "Finite element method based modelling and analysis of partial discharge acoustic wave propagation in an oil-filled power transformer," in *Proc. IEEE 4th Int. Conf. Condition Assessment Techn. Electr. Syst. (CATCON)*, Nov. 2019, pp. 1–5.
[23] Z. Wang, C. Gao, L. Zheng, J. Ren, W. Wang, Y. Zhang, and S. Han, "FEM simulation and test verification of PD ultrasonic signal propagation in a power transformer model," *J. Electr. Eng. Technol.*, vol. 16, no. 1, pp. 449–457, Jan. 2021.
[24] H.-Y. Zhou, G.-M. Ma, M. Zhang, H.-C. Zhang, and C.-R. Li, "A high sensitivity optical fiber interferometer sensor for acoustic emission detection of partial discharge in power transformer," *IEEE Sensors J.*, vol. 21, no. 1, pp. 24–32, Jan. 2021.
[25] X. Wang, B. Li, H. T. Roman, O. L. Russo, K. Chin, and K. R. Farmer, "Acousto-optical PD detection for transformers," *IEEE Trans. Power Del.*, vol. 21, no. 3, pp. 1068–1073, Jul. 2006.

[26] C. Gao, W. Wang, S. Song, S. Wang, L. Yu, and Y. Wang, "Localization of partial discharge in transformer oil using Fabry–Pérot optical fiber sensor array," *IEEE Trans. Dielectr. Electr. Insul.*, vol. 25, no. 6, pp. 2279–2286, Dec. 2018.
[27] Z. Zhang, J. Lei, W. Chen, T. Yang, Y. Song, K. Wu, and F. Liu, "Oil-paper insulation partial discharge ultrasonic multifrequency sensing array based on fibre-optic Fabry–Pérot sensor," *High Voltage*, vol. 7, no. 2, pp. 325–335, Apr. 2022.
[28] B. Dong, M. Han, L. Sun, J. Wang, Y. Wang, and A. Wang, "Sulfur hexafluoride-filled extrinsic Fabry–Pérot interferometric fiber-optic sensors for partial discharge detection in transformers," *IEEE Photon. Technol. Lett.*, vol. 20, no. 18, pp. 1566–1568, Sep. 15, 2008.
[29] J. Posada-Roman, J. A. Garcia-Souto, and J. Rubio-Serrano, "Fiber optic sensor for acoustic detection of partial discharges in oil-paper insulated electrical systems," *Sensors*, vol. 12, no. 4, pp. 4793–4802, Apr. 2012.
[30] F. Predl, W. Guo, S. Hoek, and M. Krger, "Combining acoustic and electrical methods to locate partial discharge in a power transformer," in *Proc. IEEE 11th Int. Conf. Properties Appl. Dielectr. Mater. (ICPADM)*, Jul. 2015, pp. 424–427.
[31] S. M. Markalous, S. Tenbohlen, and K. Feser, "Detection and location of partial discharges in power transformers using acoustic and electromagnetic signals," *IEEE Trans. Dielectr. Electr. Insul.*, vol. 15, no. 6, pp. 1576–1583, Dec. 2008.
[32] S. Coenen and S. Tenbohlen, "Location of PD sources in power transformers by UHF and acoustic measurements," *IEEE Trans. Dielectr. Electr. Insul.*, vol. 19, no. 6, pp. 1934–1940, Dec. 2012.
[33] Y. Lu, X. Tan, and X. Hu, "PD detection and localisation by acoustic measurements in an oil-filled transformer," *IEE Proc.-Sci., Meas. Technol.*, vol. 147, no. 2, pp. 81–85, Mar. 2000.
[34] Y.-B. Wang, D.-G. Chang, Y.-H. Fan, G.-J. Zhang, J.-Y. Zhan, X.-J. Shao, and W.-L. He, "Acoustic localization of partial discharge sources in power transformers using a particle-swarm-optimization-route-searching algorithm," *IEEE Trans. Dielectr. Electr. Insul.*, vol. 24, no. 6, pp. 3647–3656, Dec. 2017.
[35] P. Jitjing, P. Sritong, C. Suwanasri, and T. Suwanasri, "The comparative study of PD detecting in power transformer model according to acoustic emission and IEC270 standard method," *Appl. Mech. Mater.*, vol. 781, pp. 312–315, Aug. 2015.
[36] J. J. Moré, "The Levenberg–Marquardt algorithm: Implementation and theory," in *Numerical Analysis* (Lecture Notes in Mathematics). Berlin, Germany: Springer, 1978, pp. 105–116.
[37] S. M. Markalous, S. Tenbohlen, and K. Feser, "New robust non-iterative algorithms for acoustic PD-localization in oil/paper-insulated transformers," in *Proc. 14th Int. Symp. High Voltage Eng.*, 2005, pp. 1–6.

HAMIDREZA BESHARATIFARD received the B.S. and M.S. degrees in electrical engineering from the Qom University of Technology, Iran, in 2019 and 2021, respectively. His research interests include condition monitoring of power apparatus, high-voltage insulation, and high-voltage testing.

SAEED HASANZADEH received the M.Sc. and Ph.D. degrees in electrical engineering from the University of Tehran (UT), Tehran, Iran, in 2006 and 2012, respectively. His M.Sc. thesis and Ph.D. dissertation have been conducted in high voltage engineering and wireless power transfer (WPT). In 2013, he joined the Department of Electrical and Computer Engineering, Qom University of Technology, as an Assistant Professor. Since 2018, he has been the Dean of the Department of Electrical and Computer Engineering (ECE), Qom University of Technology. He was also recognized as an Outstanding Lecturer at the Qom University of Technology, in 2020. His current research interests include power electronics, electrical machines, wireless power transfer, and high-voltage engineering. He is a member of the Editorial Board of the Power Electronics Society of Iran (PELSI) and a TPC Member of the IEEE Power Electronics and Drives: Systems and Technologies Conference (PEDSTC). He was a recipient of the Top Research Prize of the Qom University of Technology, in 2019.

EHSAN HEYDARIAN-FORUSHANI received the M.Sc. degree in electrical engineering from Tarbiat Modares University, Tehran, Iran, in 2013, the Ph.D. degree in electrical engineering from the Isfahan University of Technology, Isfahan, Iran, in 2017, the first Postdoctoral degree from the Isfahan University of Technology, in 2019, and the second Postdoctoral degree from Aix-Marseille University, Marseille, France. He was a Visiting Researcher with the University of Salerno, Salerno, Italy, from 2016 to 2017. As an industrial experience, he was worked at Esfahan Electricity Power Distribution Company (EEPDC), from 2018 to 2021. He is currently an Assistant Professor with the Qom University of Technology, Qom, Iran. He was also worked on an EU-funded H2020 Project Virtual Power Plant for Interoperable and Smart isLANDS (VPP4ISLANDS), a 7.2-million-euro project involving 19 academic and industry partners with Aix-Marseille University. His research interests include power system flexibility, active distribution networks, renewables integration, demand response, smart grids, and electricity market.

S. M. MUYEEN (Senior Member, IEEE) received the B.Sc. degree in electrical and electronic engineering from the Rajshahi University of Engineering and Technology (RUET), formerly known as the Rajshahi Institute of Technology, Bangladesh, in 2000, and the M.Eng. and Ph.D. degrees in electrical and electronic engineering from the Kitami Institute of Technology, Japan, in 2005 and 2008, respectively. He is currently working as a Full Professor with the Department of Electrical Engineering, Qatar University. He has published more than 250 articles in different journals and international conferences, and seven books as the author or an editor. His research interests include power system stability and control, electrical machine, FACTS, energy storage systems (ESSs), renewable energy, and HVDC systems. He is a fellow of Engineers Australia. He is serving as an Editor/Associate Editor for many prestigious journals from IEEE, IET, and other publishers, including IEEE TRANSACTIONS ON ENERGY CONVERSION, IEEE POWER ENGINEERING LETTERS, *IET Renewable Power Generation*, and *IET Generation, Transmission and Distribution*. He has been a keynote speaker and an invited speaker at many international conferences, workshops, and universities.